Conf-911003--22

UCRL- JC-108915
PREPRINT

Deformation and Fracture Behavior of Tungsten-5% Rhenium and Unalloyed Tungsten Under Dynamic Tensile Loading

D. H. Lassila
M. M. LeBlanc

THIS PAPER WAS PREPARED FOR SUBMITTAL TO
ASM/TMS Fall Meeting
October 23-25, 1991
Cincinnati, Ohio

October 10, 1991

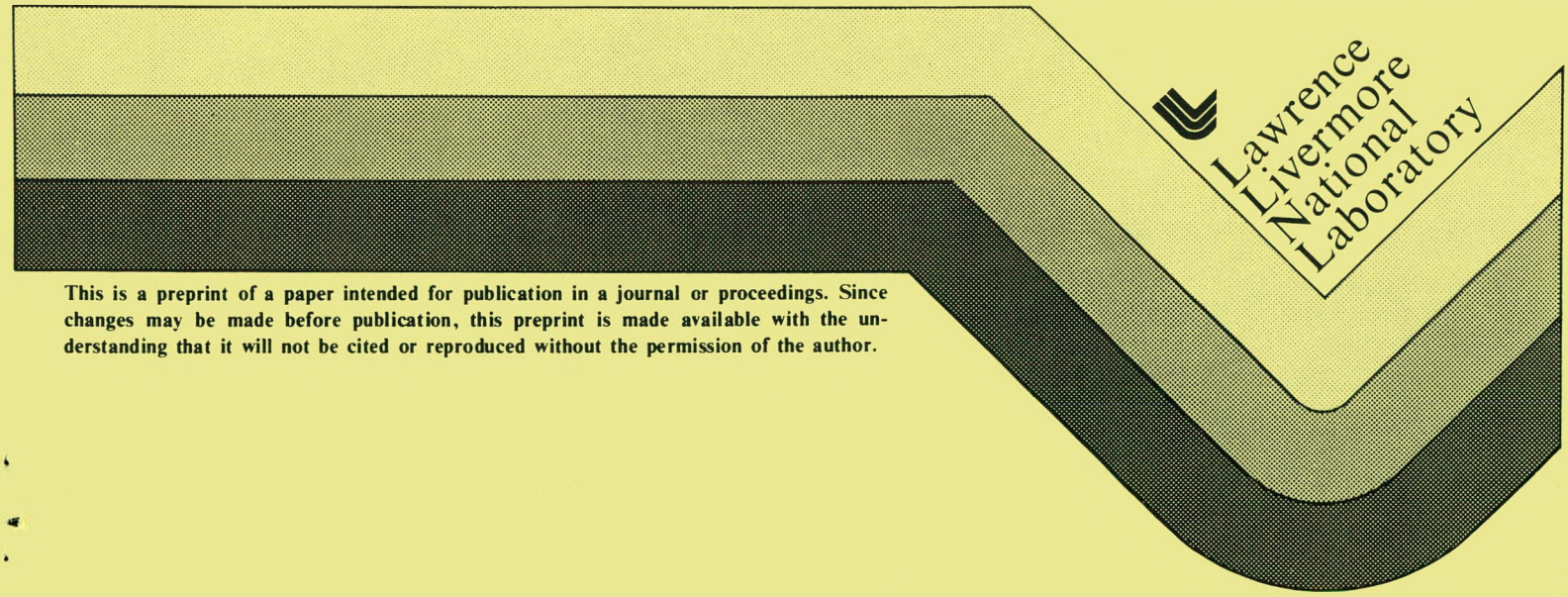

DISCLAIMER

Deformation and Fracture Behavior of Tungsten-5% Rhenium and Unalloyed Tungsten Under Dynamic Tensile Loading

UCRL-JC--108915

DE92 007306

D. H. Lassila and M. M. LeBlanc

University of California
Lawrence Livermore National Laboratory
Livermore, California 94551

ABSTRACT

The deformation behavior and ductile-brittle transition temperatures (DBTT) of unalloyed tungsten and a tungsten-5% rhenium alloy were investigated under quasi-static and dynamic loading conditions. Both test materials were tested in the warm-worked/wrought microstructural state. Testing was performed over a range of temperatures from 23° C to 450° C. In this work, the DBTT was defined as the test temperature at which ductile (necking) failure of the test sample is expected. Consistent with other studies reported in the literature, the tungsten-5% rhenium alloy has a considerably lower DBTT than the unalloyed material under quasi-static loading. In contrast, under dynamic loading the tungsten-5% rhenium alloy and the unalloyed material have similar ductile-brittle transition behavior.

INTRODUCTION

The change in tensile fracture mode from brittle (intergranular or transgranular cleavage) to ductile rupture (necking) with increasing temperature is a well established phenomenon in BCC metals such as tungsten [1,2]. This transition in fracture behavior is known to be dependent on microstructure [3,4], alloying additions [5-9], interstitial impurity concentrations [3,10] and mechanical effects such as surface conditions [11] and loading rate [12]. A single temperature, referred to as the ductile-brittle transition temperature (DBTT), is generally used to characterize the transition in fracture behavior. Often the DBTT is determined using three-point bend testing by characterizing the transition from test temperatures which result in no apparent macroscopic plastic deformation prior to brittle fracture to test temperatures which result in some extent of plastic deformation without failure. The DBTT, determined in this manner, is somewhat arbitrary and provides only an approximate indication of transition behavior because the transition from fully brittle to ductile fracture behavior occurs over a range of temperature [13,14] and the ductile fracture mode generally does not occur under three-point bend loading. Additionally, under dynamic loading conditions (impact loading) the three-point bend test can be problematic due to geometrical constraints associated with this loading method [14]. Other test methods, such as uniaxial tensile testing, must be employed to define and understand the ductile-brittle transition under dynamic loading .

In previous work, the ductile-brittle transition behavior of a warm-forged tungsten material was determined using three-point bend testing under quasi-static loading conditions [13]. In the current work, we investigate the quasi-static and dynamic deformation and fracture behavior of this material and a warm-swaged tungsten-5% rhenium alloy. We first present the material microstructures, quasi-static test technique and the tensile split Hopkinson pressure bar (SHBP) technique which was used to test the materials under dynamic loading. Subsequently, the deformation and failure modes of the test materials under quasi-static and dynamic conditions are presented. The test data is then used to assess the ductile-brittle transition behavior.

EXPERIMENTAL

Unalloyed tungsten was processed by axially forging (90% reduction) powder metallurgy billets supplied by GTE Sylvania (K-100 specification) at a temperature just below the recrystallization temperature. Prior to warm-forging, the billets were compacted by isostatic pressing at a pressure of 270 MPa and then sintered in a dry hydrogen atmosphere at 2100° C for 30 hours. The tungsten-5% rhenium test material was prepared by first sintering a cold compact in a hydrogen atmosphere at 2300° C. The sintered bar was then swaged in steps at temperatures ranging from 1300° C to 950° C. The total work imparted to the sintered material during this process is estimated to be approximately 60%.

The results of chemical analyses of the test materials, which were performed using spark-source mass

Table 1 Bulk Impurity Concentrations in Tungsten Samples
(Weight Percent)

	C	H	O	N	S	All other impurities*
W	0.002	0.0001	<0.001	<0.001	<0.001	212 wt ppm
W-5Re	0.002	0.0002	0.002	<0.001	0.004	not available

*May include: Al, Cr, Fe, Ca, Ti, Cu, Mg, Ni, Mn, Zr, and Be. All other elements were below detection limits (<0.001).

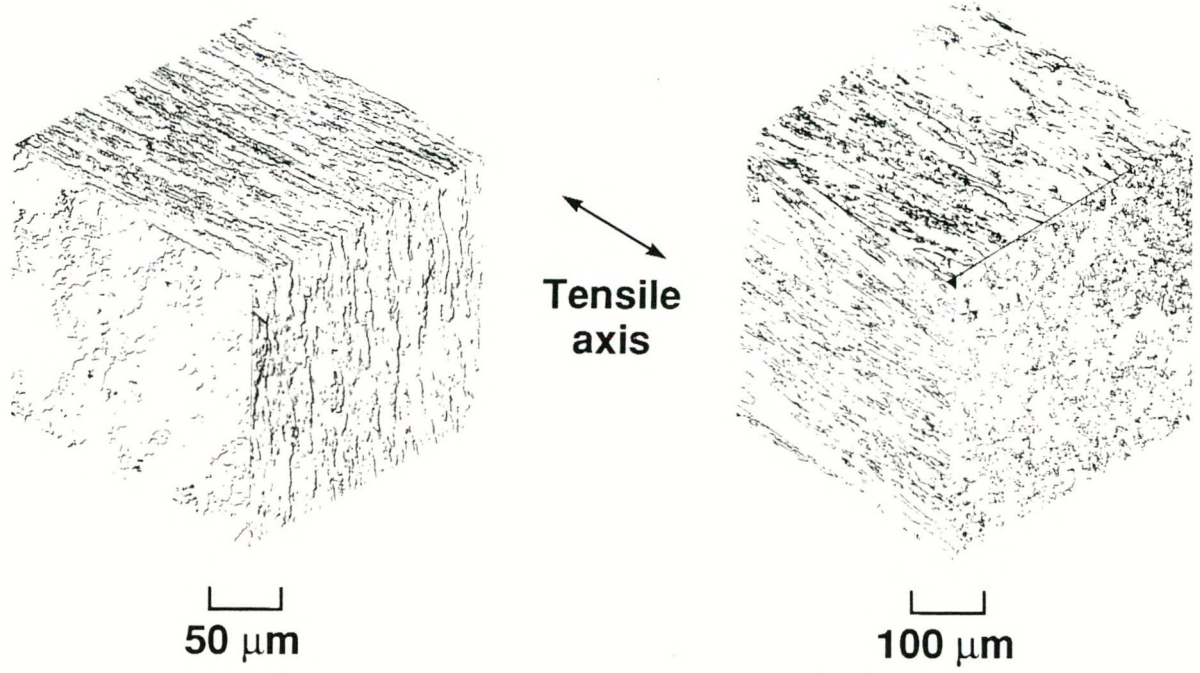

Figure 1. Microstructures of test materials relative to the tensile axis of the test sample. (a) Unalloyed tungsten. (b) Tungsten-5% rhenium.

spectroscopy and gas fusion analysis, are given in Table 1. Optical light micrographs shown in Figures 1-a and 1-b illustrate the wrought microstructures of the test materials. Other work on fracture behavior of tungsten suggests warm working destroys the continuity of the relatively low-energy crack initiation and fracture paths along grain boundaries, resulting in lower DBTTs. Because of this, we believe the test material microstructures may be near optimum in terms of achieving low temperature ductile-brittle transition behavior.

Flat test samples, with small integral gage marks, were used for both the quasi-static and dynamic tensile tests. The geometry of the test sample is shown in Figures 2 and 3-a. The samples were electrical discharge machined (EDM) from the study materials with the tensile axes oriented parallel to the elongated microstructure (Figure 1). The flat faces of the samples were mechanically polished and then the entire sample was electropolished in a 2% NaOH solution using a 7 to 10 volt potential for about 120 seconds. Strips of copper foil, 125 μm thick, were brazed to the gripping areas of the sample in a vacuum at 900° C. These copper surfaces allowed the serrated grips of the tensile test fixture (Figure 3-a) to mechanically fasten to the sample. Deformation of the copper gripping surface caused by fastening the sample in the grips is shown in Figure 2.

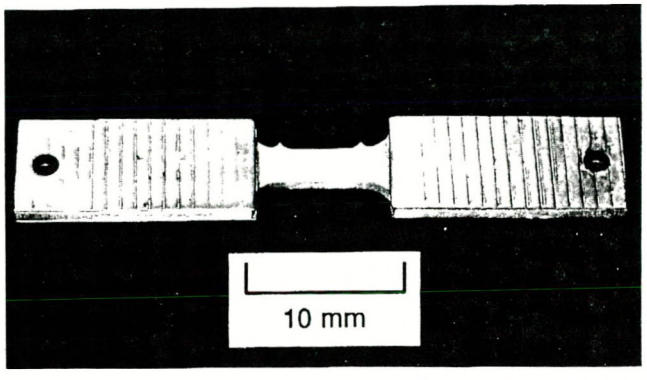

Figure 2. Photograph of the test sample showing the copper foil that was brazed to the grip surfaces. The serrated grips left impressions in the copper foil.

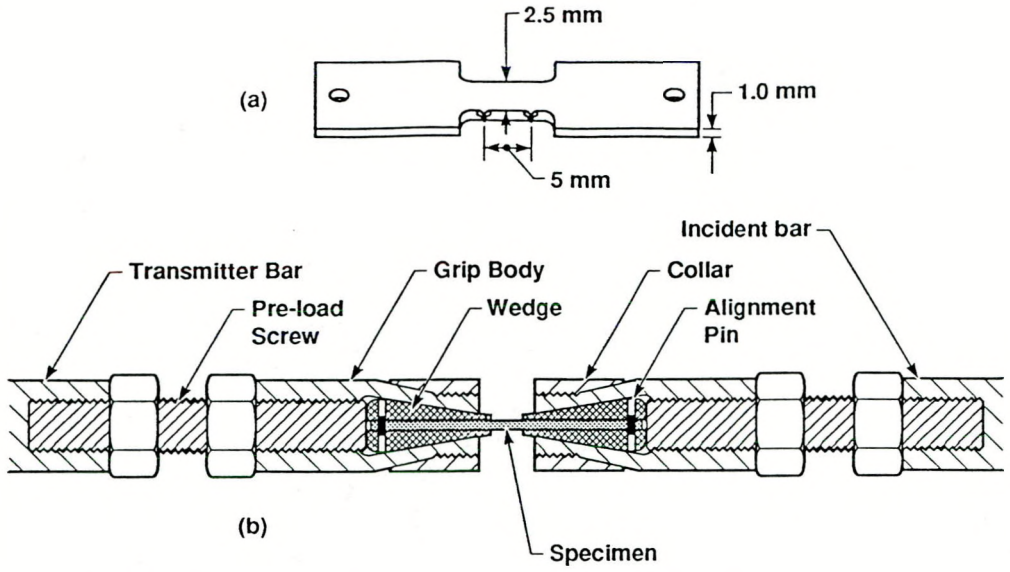

Figure 3. (a) Tensile sample without copper foil attached to the grip areas. (b) Cross-sectional view of the tensile SHPB grips.

The quasi-static tests were performed using a screw driven test machine at an initial strain rate of 10^{-3} s^{-1}. Elevated temperature testing was performed using a forced-air environmental chamber. A video camera was used to record the deformation of the sample. The elongation of the test sample during deformation was determined by measuring the displacement of the gage marks on the video image. A standard load cell was used to measure loading of the test samples, which was used together with the strain information from the video tapes to generate engineering stress-strain plots.

The dynamic tensile tests were performed using the split Hopkinson pressure bar (SHPB) technique, which is described in detail elsewhere [15]. The average strain-rate achieved using this test technique is typically 8500 s^{-1}, but does vary to some extent due to variation in the constitutive behavior of the test sample. A cross-sectional drawing of the wedge type grips developed for the testing of 1.0 mm thick sheet material is shown in Figure 3-b. A schematic of the test hardware and associated electronics is shown in Figure 4. Deformation and failure of the test samples was recorded by silhouette photographs taken at approximately 1.5 us intervals using a high speed framing camera. Representative framing camera images showing uniform elongation, ductile necking and fracture of a test sample are shown in Figure 5. Strain as a function of time, as shown in Figure 6, was extracted from the framing camera record by measuring the displacement of the gage marks off of each frame using an optical comparator. Stress in the test sample as a function of time (Figure 7) was determined using the wave-form recorded using the transmitter bar. The stress and strain records (Figures 6 and 7) are phased in time using fiducial indications on the framing camera record to produce stress-strain curves.

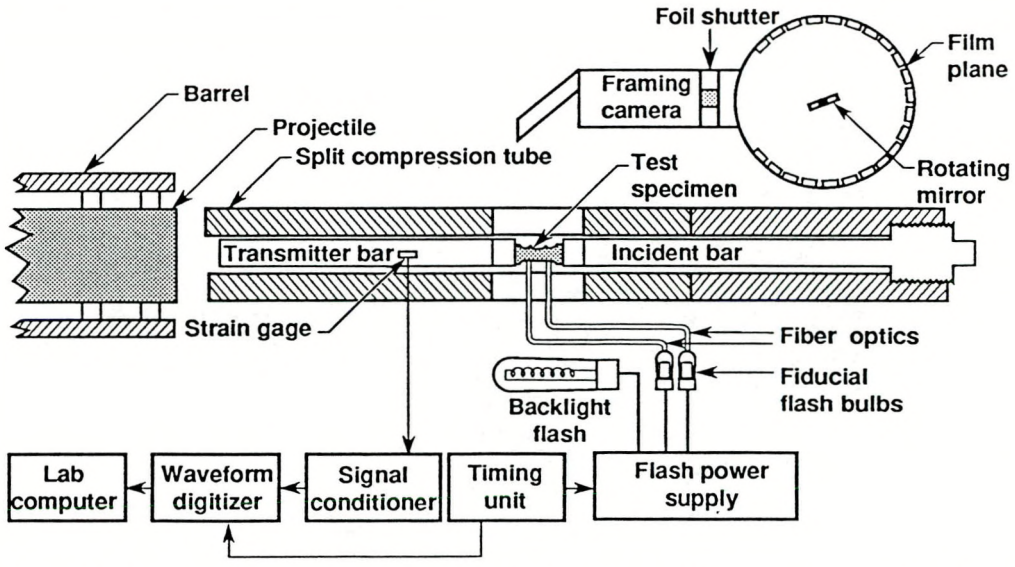

Figure 4. Schematic of the tensile SHBP test hardware, associated electronics and high speed framing camera.

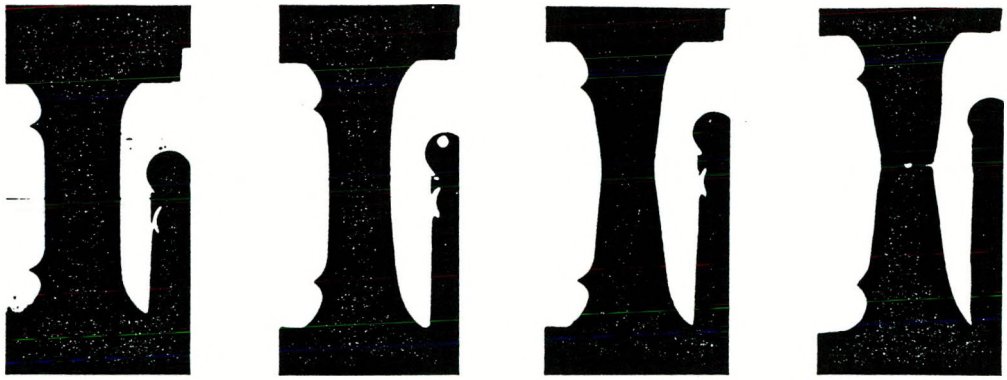

Figure 5. Framing camera images of a tungsten-5% rhenium SHBP sample taken while being deformed at 330° C. The fiber optics which are used for fiducial marks are seen to the left of the images.

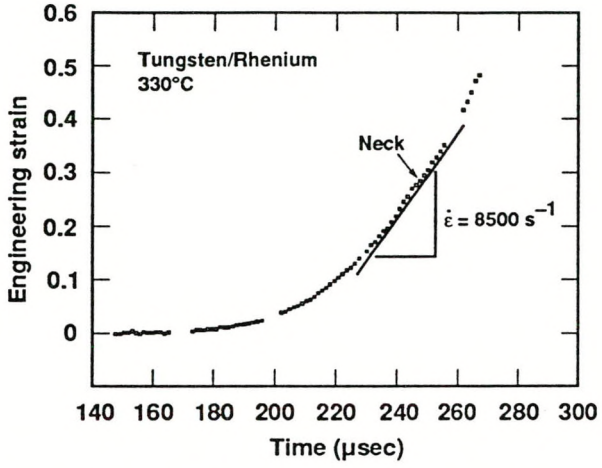

Figure 6. Plot of strain versus time which was determined from gage mark displacements measured on the framing camera photographs.

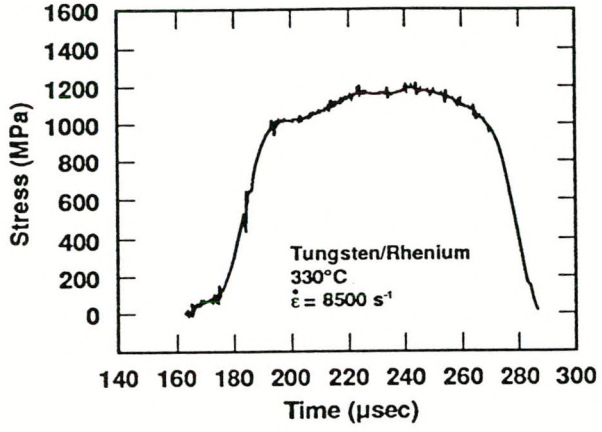

Figure 7. Engineering stress in the test sample versus time calculated using the transmitter bar wave-form.

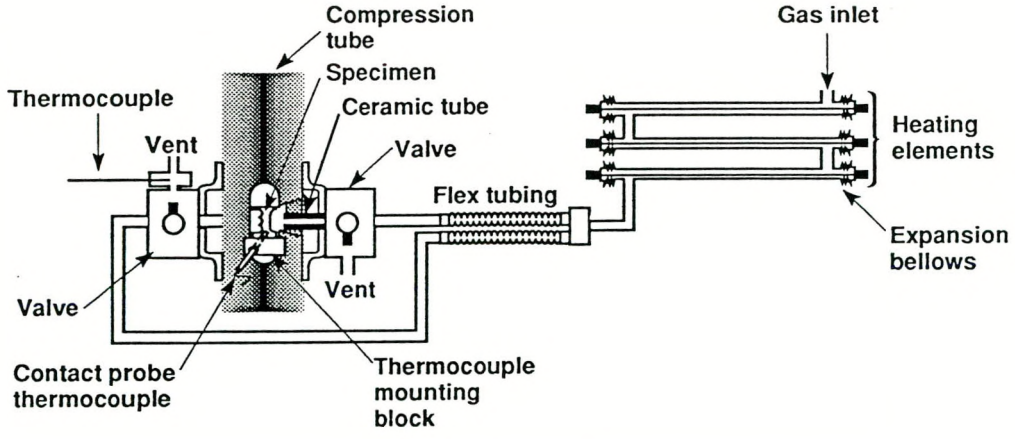

Figure 8. Diagram showing the hardware associated with elevated temperature tensile SHBP testing. Testing can be performed at temperatures up to 400° C using this heating technique.

The stress versus time information extracted from the wave-form measured by the transmitter bar can be inaccurate due to deformation in the grip regions of the test sample and extraneous wave reflections in the grips [15]. This leads directly to uncertainties in the accuracy of the stress-strain behavior. We believe that the dynamic stress-strain behavior of the test materials presented in this work are reasonably accurate because deformation of the sample remained localized in the gage section. However, we do not recommend the use of the tensile SHPB data for detailed analysis of stress-strain behavior without confirmation of the results through other testing techniques which are known to have good accuracy, such as compression SHPB tests. Because the deformation of the sample is determined by direct observation using a framing camera, strain versus time, necking and failure strains are known to be accurate.

Tensile SHPB tests were performed at elevated temperatures using a forced-gas heating system. A schematic of the heating system is shown in Figure 8. To heat a test sample, nitrogen is passed through a series of heating elements while vented away from the test sample until the gas is the proper temperature. The sample is then heated by directing the gas towards the sample. A thermocouple probe in contact with a point on the gage section was used to measure temperature of the test sample. To correct for the difference between the contact probe and the actual sample temperature and to investigate the inherent temperature gradient in the test sample, a dummy test sample was instrumented with intrinsic thermocouples at the center and ends of the gage length. The temperature gradient along the gage section was found to vary approximately $\pm 2.5°$ C at an average sample temperature of 90° C. The variation in test temperature increased with increasing sample temperature. At a sample temperature of 350° C the variation in sample temperature was found to be $\pm 12°$ C.

TENSILE TEST RESULTS

The engineering stress-strain behavior of the unalloyed tungsten under quasi-static loading is shown in Figure 9. At a test temperature of 50° C, this material exhibits brittle fracture prior to permanent plastic deformation. At a test temperature of 155° C, a significant amount of plastic deformation (8%) occurs prior to brittle fracture. Failure is initiated by localized plasticity (necking) at a test temperature of 250° C.

The engineering stress-strain behavior of the tungsten-5% rhenium alloy under quasi-static loading is shown in Figure 10. The deformation and fracture behavior of this material is similar to the unalloyed material; i.e. a transition from brittle failure to one controlled by deformation stability occurs with an increase in test temperature.

The deformation and fracture behavior of the test materials under dynamic loading was found to be analogous to the quasi-static behavior. Selected engineering stress-strain curves of the unalloyed tungsten under dynamic loading ($\dot{\varepsilon} = 8500\ s^{-1}$) are shown in Figure 11. At a test temperature of 23° C brittle fracture of the sample occurs prior to permanent plastic deformation. At a test temperature of 330° C brittle fracture also occurs, however some plastic deformation occurs prior to failure. Ductile necking, as observed on the framing camera record, initiates failure at a test temperature of 355° C. After necking begins, significant post-uniform deformation occurs prior to fracture at a strain of 29%. The deformation and fracture behavior of the tungsten-5% rhenium alloy under dynamic loading was found to be similar to the unalloyed tungsten, as indicated by the engineering stress-strain curves shown in Figure 12. Brittle fracture occurred at test temperatures up to 310° C. Ductile failure, initiated by the growth of a neck, occurred at test temperatures of 330° C and greater.

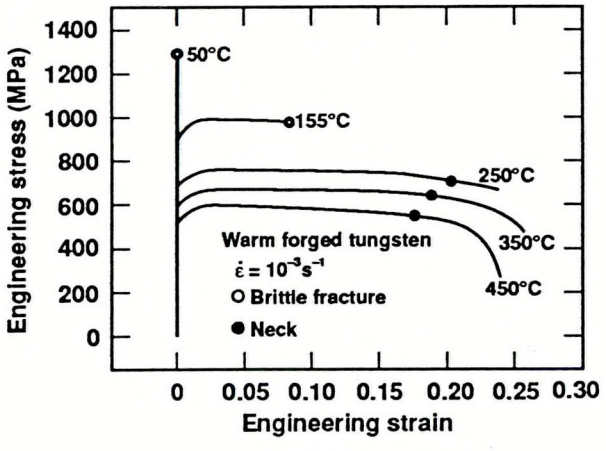

Figure 9. Engineering stress-strain behavior of the unalloyed tungsten material under quasi-static deformation.

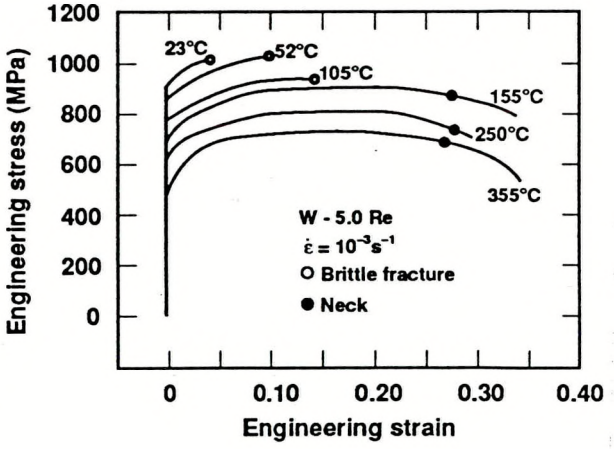

Figure 10. Engineering stress-strain behavior of the tungsten-5% rhenium material under quasi-static deformation.

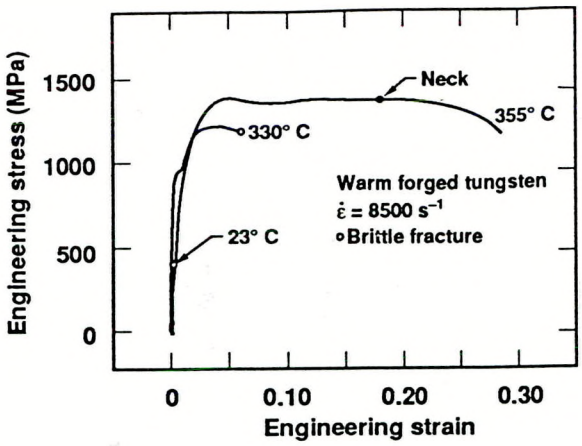

Figure 11. Engineering stress-strain behavior of the unalloyed tungsten material under dynamic loading.

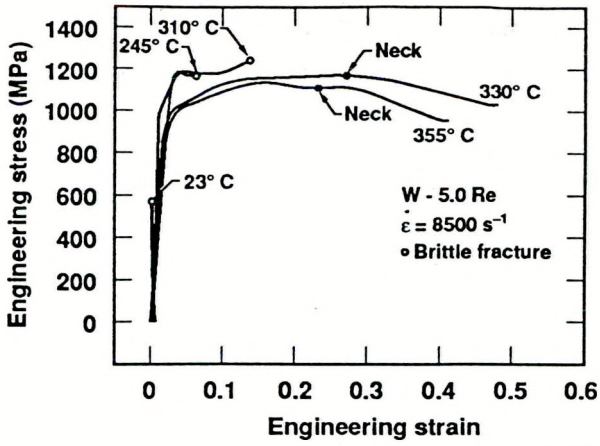

Figure 12. Engineering stress-strain behavior of the tungsten-5% rhenium material under dynamic loading.

At a given test temperature under both quasi-static and dynamic loading we find that the tungsten-5% rhenium alloy exhibits lower yield strength and higher work hardening behavior than that of the unalloyed tungsten. This result is in qualitative agreement with previous works which have reported on the effects of the alloying of tungsten with rhenium on deformation behavior [5,6,8]. Primarily due to the above differences in constitutive behavior, the tungsten-5% rhenium alloy exhibits more elongation prior to necking than the unalloyed material (at a given test temperature which results in ductile necking type failure). Analysis of the mechanics of tensile deformation in conjunction with a sufficiently detailed constitutive description of the test material will allow accurate prediction of deformation stability under quasi-static and dynamic loading [16-19], however a detailed analysis of this type is beyond the scope of this paper.

FRACTURE MORPHOLOGIES

The brittle fracture morphologies of the unalloyed tungsten and the tungsten-5% rhenium exhibited similar features. A low magnification scanning electron microscope (SEM) photo of a typical brittle fracture of a tungsten-5% rhenium tensile sample is given in Figure 13-a. A higher magnification SEM micrograph of this surface (Figure 13-b) reveals polygonal facets about 2 μm in length grouped together. Because the grain size of this material measured in the fracture plane is approximately one order of magnitude greater than the size of these features (Figure 1-b), we believe that these groups of polygonal features are related to subgrains [20]. Cleavage areas with striations are also apparent on the fracture surface of this material. In some cases, the striations fan out from a group of polygonal intergranular facets, which suggests the subgrain area acted as a cleavage fracture nucleation site.

The fracture surface features of samples which necked prior to failure appeared to be closely related to the different microstructures of test materials. A low magnification SEM photo of an unalloyed tungsten sample which necked prior to fracture is shown in Figure 13-c. In this photo and the high magnification SEM micrograph shown in Figure 13-d, lamellar features associated with the highly deformed microstructure are clearly apparent. The ductile fracture of a tungsten-5% rhenium test sample is illustrated in Figures 13-e and 13-f. The low magnification image (Figure 13-e) indicates a relatively large extent of localized plasticity occurred prior to fracture. The fibrous "woody" type fracture surface features apparent in the high magnification SEM micrograph are clearly related to the elongated microstructural features found in metallographic observations (Figure 1-b).

DUCTILE-BRITTLE TRANSITION BEHAVIOR

The value of engineering strain at which failure occurs, which we refer to as the failure strain (ε_f), is plotted versus test temperature for both test materials in Figure 14. The transitions from brittle fracture behavior to failure controlled by deformation stability (necking) occur over a range of temperature, about 150° C to 200° C, for both test materials under quasi-static and dynamic loading. In this work a single DBTT is defined which represents the temperature at which failure of the material is controlled by deformation stability. To do this, curves were drawn through the sets of data points and an intercept was determined at a value of strain approximately equal to the maximum value of ε_f. This intercept, as shown in Figure 14, is then used to define the DBTTs.

Table 2. DBTTs of test materials

Strain Rate (s^{-1})	DBTT (°C)	
	Unalloyed Tungsten	Tungsten 5% Rhenium
10^{-3}	280	150
8500	360	340
Temperature shift	80	190

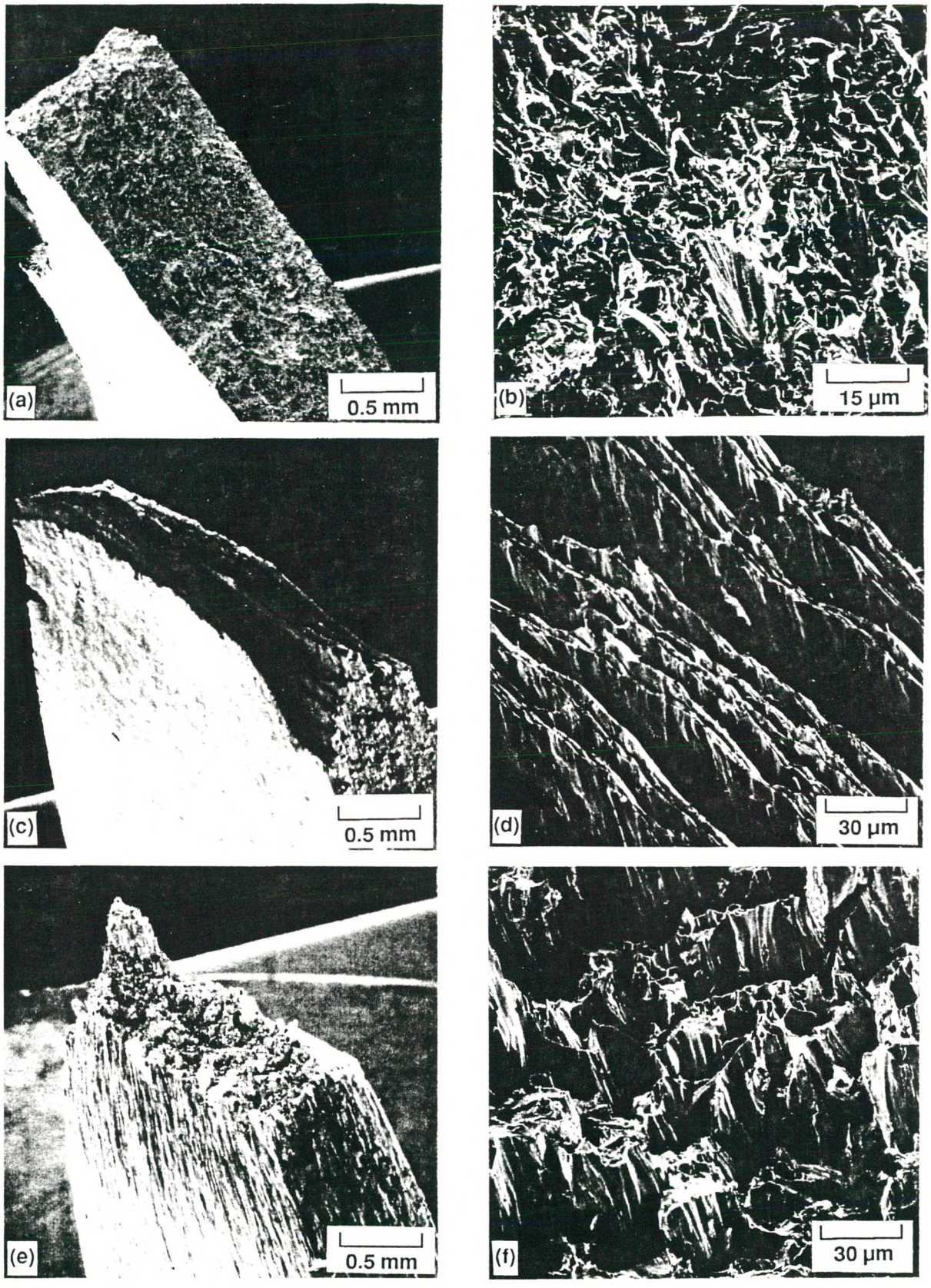

Figure 13. SEM photographs of test samples and fracture surfaces. (a) Low magnification photograph of a typical brittle fracture (tungsten-5% rhenium tested at 23° C under dynamic loading.) (b) High magnification micrograph of the fracture surface shown in Figure 13-a. (c) Ductile fracture of a unalloyed tungsten sample tested at 350° C under quasi-static loading. (d) High magnification micrograph of the fracture surface shown in Figure 13-c. (e) Ductile fracture of a tungsten-5% rhenium sample tested at 330° C under dynamic loading. (f) High magnification micrograph of the fracture surface shown in Figure 13-e.

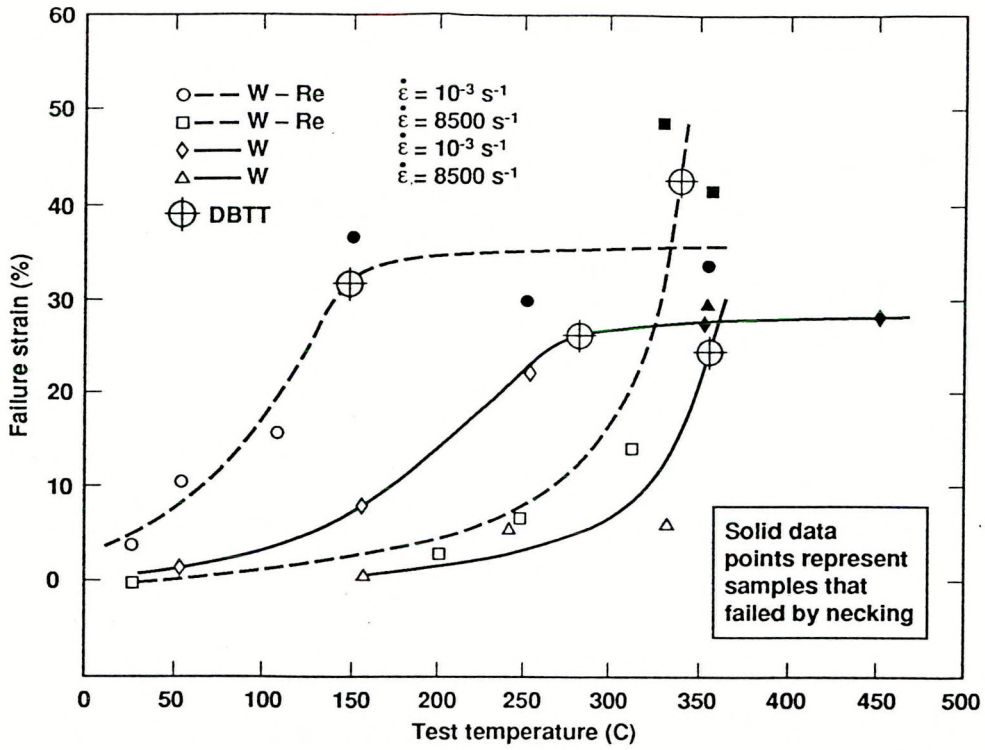

Figure 14. Failure strain versus test temperature under quasi-static and dynamic loading. As described in the text, the DBTT points represent the minimum test temperature at which ductile (necking) failure is expected. For reasons not understood, the shift temperature of the tungsten-5% rhenium is considerably greater than that of the unalloyed tungsten leading to similar ductile-brittle transition behavior and DBTTs under dynamic loading.

The DBTTs determined for the test materials are summarized in Table 2 and are based, unfortunately, on a rather limited data base. They are, however, consistent with other studies on two accounts; the DBTT for a given material is significantly higher under dynamic loading and, alloying of tungsten with rhenium lowers the DBTT under quasi-static loading. The data also points to a finding believed to be new; the difference in the DBTTs of the two test materials which is quite apparent under quasi-static loading is almost negligible under dynamic loading conditions. In other work a "temperature-shift" is defined as the difference between the DBTT under dynamic loading minus the DBTT under quasi-static loading [21]. A decrease in the temperature-shift with increase in yield strength has been observed in some ferritic structural steels [22]. This correlates with the data presented in this work, i.e. the higher strength unalloyed tungsten has a lower temperature-shift. The similarity of the behavior of these BCC metals suggests the constitutive behavior of the test material is related to the temperature-shift phenomenon, although a mechanistic understanding remains unknown.

CONCLUSIONS

The work presented on the deformation and ductile-brittle transition behavior of unalloyed tungsten and a tungsten-5% rhenium alloy yields the following conclusions:

1. The tungsten-5% rhenium alloy exhibited lower yield strength and higher work hardening than the unalloyed material under quasi-static and dynamic loading, which is in qualitative agreement with other studies. These differences in constitutive behavior lead to greater extents of uniform elongation under deformation conditions which result in ductile (necking) failure.

2. A transition from brittle fracture to failure controlled by necking occurred in both test materials with increase in test temperature, as expected. In this work, the DBTT was defined as the temperature at which ductile (necking) failure of the test sample is expected.

3. The DBTT of the tungsten-5% rhenium alloy was found to be considerably lower than that of the unalloyed tungsten under quasi-static loading. In contrast, under dynamic loading the difference in the DBTTs of the test materials was nearly zero. (The DBTTs are summarized in Table 2.)

ACKNOWLEDGMENTS

The authors would like to acknowledge the help of Ms. Betty Bowers, who helped prepare the manuscript, Mr. Robert Kershaw who performed the metallography, and Mr. Jim Yoshiyama who performed the SEM analysis.

AUSPICES

Work performed under the auspices of the U. S. Department of Energy by the Lawrence Livermore National Laboratory under contract No. W-7405-ENG-48.

REFERENCES

1. J. H. Bechtold and P. G. Shewmon, Trans. Am. Soc. Metals, 46 (1954) 397.

2. J. W. Clark, "Flow and Fracture of Tungsten and its Alloys: Wrought, Recrystallized, and Welded Conditions", Air Force Systems Command, Technical Documentary Report (April 1963), No. ASD-TDR-63-420.

3. J. R. Stephens, "Effects of Interstitial Impurities on the Low-Temperature Tensile Properties of Tungsten", Report NASA-TND 2287, (1964).

4. V. I. Trefilov and Yu. V. Milman, 12th International Plansee Seminar '89, Refractory Metals and Related Topics, Superconductors, Reutte, Tirol, Austria, May 1989, Vol. 1, (Publ: Metallwerk Plansee Gmbh, Reutte, Tirol, Austria, 1989).

5. P. L. Raffo, J. Less-Common Metals, 17 (1969), 133.

6. J. R. Stephens and W. R. Witzke, J. Less-Common Metals, 23, (1971), 325-342.

7. S. H. Whang, S. U. Kim, and D. Kapoor, "Effect of Silicon Addition in Rapidly Solidified Tungsten Alloys", 1988 International Powder Metallurgy Conference, Modern Developments in Powder Metallurgy, Vol. 19, 105-119.

8. Y. N. Podrezov, O. G. Radchenko, N. G. Danilenko, V. V. Panichkina, V. I. Gachegov, and A. B. Ol'shanskii, Soviet Powder Metallurgy and Metal Ceramics, Vol 26, No. 8(296), August, (1987), 677-679.

9. L. S. Kosachev et al., Phys. Metals, Vol 6, 2, (1985) 264.

10. G. T. Hahn, A. Gilbert and R. I. Jaffee, Refractory Metals and Alloys II, Metallurgy Society Conference Vol. 17 (Interscience, New York, London, 1962).

11. J. R. Stephens, Rev. Deformation Behavior Materials, 1, (1974) 31.

12. V. D. Barth, "Physical and Mechanical Properties of Tungsten and Tungsten-Base Alloys", (DMIC Report 127, Defense Metals Information Center, 1960).

13. "Fracture Behavior of Warm Forged and CVD Tungsten", Tungsten and Tungsten Alloys, Recent Advances, ed. A. Crowson and E. S. Chen, (Warendale, PA: The Metallurgical Society, 1991), 79-85.

14. D. H. Lassila, F. Magness, and D. Freeman, "Ductile-Brittle Transition Temperature Testing of Tungsten Using the Three-Point Bend Test", UCRL-ID-108258, Lawrence Livermore National Laboratory, (1991).

15. M. M. LeBlanc and D. H. Lassila, "Dynamic Tensile Testing of Sheet Material using the Split Hopkinson Bar Technique", in progress, Lawrence Livermore National Laboratory, (1991).

16. E. W. Hart, Acta Met. 15, (1967), 351.

17. J. D. Campbell, J. Mech. Phys. Solids, 15, (1967), 359.

18. A. Considere, Ann. Ponts Chaussees, 9, (1885), 574.

19. A. K. Gosh, J. Eng., Mat. Tech. ASME, 99, (1977), 264.

20. A. G. Imgram and H. R. Ogden, "The Effect of Fabrication History and Microstructure on the Mechanical Properties of Refractory Metals and Alloys", Defense Metals Information Center, Report 186, (1963).

21. J. M. Barsom and S. T. Rolfe, Fracture and Fatigue Control in Structures, 2nd ed. (Prentice-Hall, Englewood Cliffs, NJ, 1987).

22. A. K. Shoeman and S. T. Rolfe, Engineering Fracture Mechanics 2, (1971) 319.